Progress on the Performance Improvement of Sub-Millimetre Wave Sub-Harmonically Pumped Image-Rejection Schottky Mixers

S. P. Rea[1], B. Alderman[1], M. Henry[1], D. N. Matheson[1] and Y. Munro[2]
[1]Millimetre Technology Group, STFC RAL Space, Didcot, Oxfordshire, UK, OX11 0QX
[2]Astrium Ltd, Anchorage Road, Portsmouth, UK, PO3 5PU

***Abstract*-Recent progress on the development of sub-millimetre wave sub-harmonically pumped image-rejection mixers using Schottky diodes is presented. The paper details the performance limitations of previous devices and presents the findings of recent investigations into potential causes. Subsequent work focusing on two specific areas of the device design and assembly is described together with the resulting improvements in performance.**

I. INTRODUCTION

In recent years a number of European institutions have been developing novel sideband-separating mixers for deployment in future Earth Observation missions [1-5]. This research has been targeted predominantly at the STEAM-R instrument [6], part of the scientific payload of the PREMIER mission [7]. PREMIER, a candidate for ESA's Earth Explorer 7 mission currently undergoing Phase A industrial study, is dedicated to the investigation of chemical, dynamical, and radiative processes in the upper troposphere and lower stratosphere. STEAM-R is a passive sub-millimetre wave limb-sounding instrument which will employ a fixed array of receivers providing 14 simultaneous views of the atmospheric limb covering an altitude range of 6-28 km at mid-latitudes. The receivers will operate over the frequency range 315-355 GHz. In order to best resolve sub-millimetre wave limb emission in the upper troposphere single sideband (SSB) observations are desirable. As a result an image-rejection mixer architecture was baselined for a sub-set of the 14 receiver channels, enabling SSB observation in a compact receiver configuration.

This paper presents recent progress on the development of highly-integrated sub-harmonically pumped image-rejection mixers (SHIRMs) suitable for STEAM-R. Performance limitations of previous devices are discussed and the findings of recent investigations into potential causes are presented. Subsequent work focusing on two specific areas of the device design and assembly is described together with the resulting improvements in performance.

II. SHIRM CIRCUIT TOPOLOGIES & IMPLEMENTATION

Fig. 1 presents the generic circuit topology of a sub-harmonic image rejection mixer. The circuit comprises two

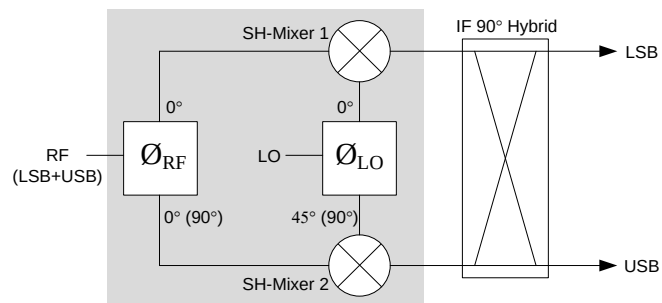

Fig. 1: Sub-harmonic Image-Rejection Mixer Circuit Topology

double sideband (DSB) sub-harmonic mixers, an RF splitter/phase shifter, an LO splitter/phase shifter and an IF quadrature hybrid. The phase offset between RF and LO inputs to the mixers is selected such that the respective sidebands are in phase-quadrature at the mixer outputs. Recombination of these signals in the IF quadrature hybrid completes the sideband separation. As shown in Fig. 1, two phasing strategies may be employed. In the first, the RF input is split with 0° phase offset and the LO is split with 45° phase offset. In the second, both RF and LO inputs are split with 90° phase offset.

The main focus of the authors has been the development of a highly-integrated micro-machined IQ mixer block comprising the DSB sub-harmonic mixers and the RF and LO splitting/phase shifting components, shown in the shaded box in Fig. 1. The image-rejection circuit is then completed by connecting a commercially available connectorized IF quadrature hybrid to the mixer IF outputs of the block. The ultimate aim is to achieve a sideband separation of 20 dB over a wide instantaneous bandwidth (2-14 GHz) without the need for corrective amplitude and/or phase tuning between the IQ mixer block and the IF quadrature hybrid. SHIRM devices comprising each of the two phasing strategies have been developed for comparative purposes and their implementation shall now be summarized. The design procedure for these devices has been previously reported [1-3].

SHIRM A: $Ø_{RF}=0°$, $Ø_{LO}=45°$

In this architecture, shown in Fig. 2, the RF input signal is split in-phase using a 3-port E-plane waveguide splitter in WR-2.8. The LO signal is split with the introduction of a 45° phase

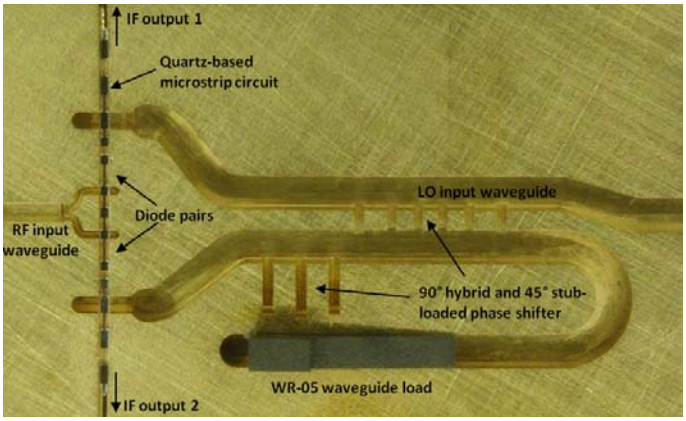

Fig. 2: Internal View of SHIRM A: $Ø_{RF}$=0°, $Ø_{LO}$=45°

offset using a branch-line quadrature hybrid followed by a 45° stub-loaded phase shifter, both in WR-5. The isolated port of the branch-line hybrid is terminated in a waveguide load machined from Eccosorb MF-116 material from Emerson & Cuming. The two DSB sub-harmonic mixer circuits are implemented on a single piece of suspended quartz-based microstrip. The RF and LO signals are coupled to each DSB mixer circuit via E-plane probes. An anti-parallel pair of planar GaAs Schottky diodes fabricated at RAL [8] is flip-chip mounted onto the gold track of each mixer circuit. Optimized filtering and matching elements ensure efficient coupling of the signals to and from the diodes. The centre of the quartz microstrip line is RF/DC grounded to the block using conductive epoxy and the IF outputs are coupled from the opposite ends via additional quartz transmission lines and K-type connectors. The device is machined using the common split-block technique.

SHIRM B: $Ø_{RF}$=90°, $Ø_{LO}$=90°

In this architecture, shown in Fig. 3, the RF and LO input signals are split with the introduction of a 90° phase offset using branch-line quadrature hybrids in WR-2.8 and WR-5 respectively. The isolated ports of both hybrids are terminated using waveguide loads of the same geometry and material as before. The implementation of the DSB sub-harmonic mixers is identical to SHIRM A.

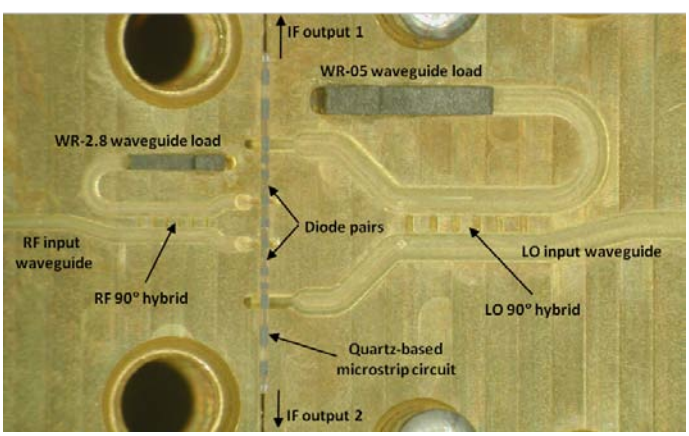

Fig. 3: Internal View of SHIRM B: $Ø_{RF}$=90°, $Ø_{LO}$=90°

The micro-machined block of either architecture has a volumetric envelope of 20 mm × 20 mm × 20 mm with UG/387 flanges incorporated for the RF and LO inputs.

III. Initial Test Results

Laboratory testing of the SHIRM devices has primarily focused on two key parameters: the sideband rejection and the SSB receiver noise temperature. Tests have been performed for IF bandwidths of 2-8 GHz and 6-14 GHz. The test procedure for determining these parameters [9] requires a Y-factor measurement to determine the DSB receiver noise temperature at each of the receiver IF outputs. Then, a narrow tone is injected into the RF port of the device and tuned within the upper and lower sidebands such that the down-converted tones correspond to the same IF output frequency. The ratio of the down-converted tones is calculated at each of the receiver outputs. This process is repeated for the desired resolution across the IF bandwidth and the measured results used to extract the sideband rejection and SSB receiver noise temperature. The rejection, in decibels, is given by:

$$R_{LSB}=10log(G_{1,LSB}/G_{1,USB}) \quad (1)$$

$$R_{USB}=10log(G_{2,USB}/G_{2,LSB}) \quad (2)$$

where $G_{n,m}$ is the conversion (power) gain of the device from each RF input sideband (LSB or USB) at each IF output port (1 or 2).

The LO chain used to pump the SHIRM comprises a W-band Gunn diode oscillator followed by an isolator, rotary vane variable attenuator and a D154 166 GHz frequency doubler from VDI. The IF bandwidth of the receiver is fixed through selection of the IF quadrature hybrid, connectorized devices from Krytar, and the subsequent IF chain components. The noise temperatures of the IF chains, excluding the IF hybrids, are 70 K and 133 K for 2-8 GHz and 6-14 GHz respectively. The amplitude and phase imbalance of the IF hybrids contributes to the overall circuit imbalance thus limiting the level of sideband rejection that can be achieved. The hybrids contribute amplitude (phase) imbalances of ±0.35 dB (±3°) at 2-8 GHz and ±0.4 dB (±5°) at 6-14 GHz. Initially the injected tone was provided by mixing two ~1.55 μm laser sources in a RAL photo-mixer [10]. More recently, a WR-2.8 comb generator from VDI driven by an Anritsu MG3694B synthesizer has been used.

SHIRM A: $Ø_{RF}$=0°, $Ø_{LO}$=45°

The initial sideband rejection performance of this architecture is presented in Fig. 4 [1]. Measurements were made at three LO input frequencies covering the RF bandwidth 318-362 GHz. This device was optimized to operate over a broad LO frequency range. The device provides levels of sideband rejection in the range 7-24 dB. Best performance is achieved at LO=174 GHz, were the average level of sideband rejection is 18.9 dB (R_{LSB}) and 19.6 dB (R_{USB}). Poorest performance is achieved at LO=170 GHz, were the average

level of sideband rejection is 11.2 dB (R_{LSB}) and 11.4 dB (R_{USB}). A SSB receiver noise temperature between 3300-3800 K and 4000-5400 K was achieved for IF bandwidths of 2-8 GHz and 6-14 GHz respectively.

To further understand the source of imbalance within the micro-machined IQ mixer block, independent tests were performed on SHIRM A using a digital correlator backend instead of the analogue quadrature hybrid component [11]. The digital correlator has the capability of combining two input signals with a virtual ±90° phase shift, corresponding to a digital implementation of the analogue quadrature hybrid. As this combination can be done ideally (i.e. with no amplitude or phase imbalance) it is possible to determine the amplitude and phase imbalance of the micro-machined IQ mixer block alone. The imbalance of the block was measured for a number of LO input frequencies over a narrow IF bandwidth (500 MHz), limited by the sampling rate of the analogue-to-digital converters in the digital correlator. The results show a maximum amplitude and phase imbalance of 2 dB and 35° respectively, indicating that phase imbalance within the IQ mixer block is the main factor limiting performance.

SHIRM B: $Ø_{RF}=90°$, $Ø_{LO}=90°$

The initial sideband rejection performance of this architecture is presented in Fig. 5. Measurements are again shown for three LO input frequencies, this time covering the RF bandwidth 318-350 GHz. This device was optimzed for an LO frequency of 167 GHz, hence the different LO test frequencies compared to SHIRM A. The device provides levels of sideband rejection in the range 5.4-25.3 dB. Best performance is achieved at LO=166 GHz, were the average level of sideband rejection is 17.7 dB (R_{LSB}) and 17.2 dB (R_{USB}). The performance is quite similar for LO frequencies of 167 GHz and 168 GHz, with slightly poorer performance at LO=168 GHz, were the average level of sideband rejection is 9.6 dB (R_{LSB}) and 9.9 dB (R_{USB}). A SSB receiver noise temperature between 3200-4300 K and 4300-5800 K was achieved for IF bandwidths of 2-8 GHz and 6-14 GHz respectively.

IV. Identification of Factors Limiting Performance

The initial test results of the two SHIRM architectures has shown that a sideband rejection of up to ~20 dB can be achieved over a broad IF bandwidth. However the results show that the level of sideband rejection can degrade sharply with a relatively small change in LO frequency. Additional tests undertaken on SHIRM A using a digital correlator backend indicate that a phase imbalance within the micro-machined IQ mixer block is the dominant source of imbalance. In order to improve the performance of the two SHIRM units it was necessary to find and correct the cause. The initial test results give a strong hint of one such source: the sensitivity of the level of sideband rejection to small changes in LO frequency suggests the presence of standing waves within the LO splitting/phase shifting network of each device. This effect is strongly indicative of a poor termination in the isolated port of

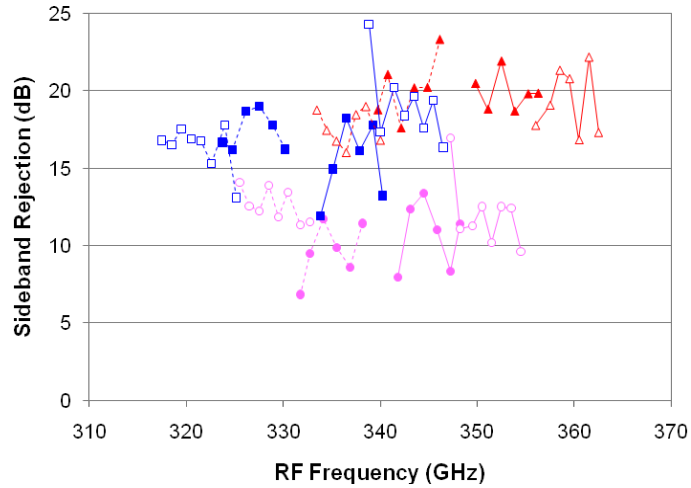

Fig. 4: Measured Sideband Rejection Performance of SHIRM A as a Function of RF Freqeuncy. Filled markers IF=2-8 GHz, empty markers IF=6-14 GHz. Dotted lines show R_{LSB} and continuous lines show R_{USB}. Blue square markers for LO=166 GHz, pink round markers for LO=170 GHz, red triagular markers for LO=174 GHz.

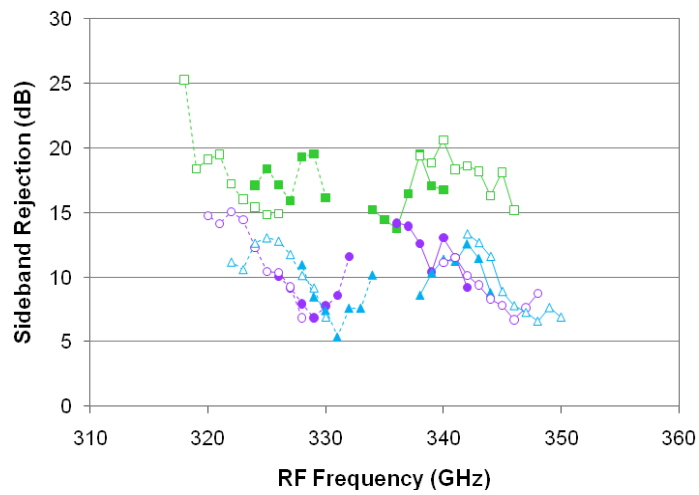

Fig. 5: Measured Sideband Rejection Performance of SHIRM B as a Function of RF Freqeuncy. Filled markers IF=2-8 GHz, empty markers IF=6-14 GHz. Dotted lines show R_{LSB} and continuous lines show R_{USB}. Green square markers for LO=166 GHz, purple round markers for LO=167 GHz, indigo triagular markers for LO=168 GHz.

the LO quadrature hybrid, whereby partially reflected LO signals from each of the DSB mixers are causing a frequency-dependent degradation in the amplitude and phase balance of the network. The investigation and resolution of this problem is described below.

Uncertainties associated with the manufacturing and assembly processes also contribute to imbalance in the IQ mixer blocks. In isolation, these have a relatively minor effect on circuit imbalance, but their combined effect may be more significant and is difficult to calculate. Their effect can at best be minimised through tolerance analysis and attention to detail throughout the development process. For example, manufacturing tolerances in the split-blocks will create a departure from the optimized 3D electromagnetic models. Tolerances are particularly critical for the smaller features such

as the branch-lines of the quadrature hybrids. The depth of the electroplated gold layer is taken into account when machining these.

Another source of imbalance is the variation in performance of the Schottky diodes. This effect is minimised by selecting diodes which have similar DC parameters. A range of electrical and reliability tests on control batches of anti-parallel Schottky diodes fabricated at RAL has provided statistical data on the variation of key diode parameters. With this information, modelling of the SHIRM with a number of mismatched diode scenarios has shown this to be a minor source of circuit imbalance given the repeatability of the fabrication process.

The assembly method currently used to mount the quartz-based microstrip transmission lines into the block has been examined. The process involves gluing two outer lines into a channel in the bottom half of the split-block. The outer ends of these lines are connected to K-type connectors for the IF outputs. The centre quartz line, containing the DSB mixer circuits, is inverted and also mounted into the channel in the bottom half of the split-block. The centre line is supported at both ends by the outer quartz lines and in the centre by a 200 μm wide plinth in the channel. This also acts as the RF/DC ground for the DSB mixers, see Fig. 6. The centre quartz line is electrically connected at the three points using conductive epoxy. The centre connection is the most critical as the millimetre wave LO and RF signals are present in this part of the circuit. Analysis has shown that any asymmetry in this electrical connection creates a phase imbalance in the circuit. However as Fig. 6 shows, it is impossible to visually determine the symmetry of the epoxy connection as the epoxy is masked by the gold track of the centre quartz line. Furthermore, any bowing of the centre quartz line during curing of the epoxy may adversely affect the symmetry of the connection. In view of this, a method for grounding the centre quartz line in this critical position without the need for conductive epoxy has been developed. Section VI examines the phase imbalance that can be created by an asymmetrical RF/DC ground connection between the two DSB mixers and presents a beam-lead based grounding method to ensure a symmetrical ground.

V. Investigation of Waveguide Load Performance

Independent tests of the return loss of the waveguide loads currently in use in the SHIRM units has recently been made possible after an upgrade of test equipment at RAL. The initial design employed, Load 1, was based on a scaled version of a WR-10 design employing a double E/H plane taper presented in [12], however an initial misinterpretation of this geometry resulted in a design comprising a single taper in the H-plane. Two additional load geometries have also been tested: the correct double-taper geometry from [12], Load 2, and a geometry comprising a single taper in the E-plane, Load 3. The geometries are shown in the inset of Fig. 7. Each of these geometries was machined in Eccosorb MF-116 and MF-112 from Emerson & Cuming for accommodation in WR-5 and WR-2.8 waveguide.

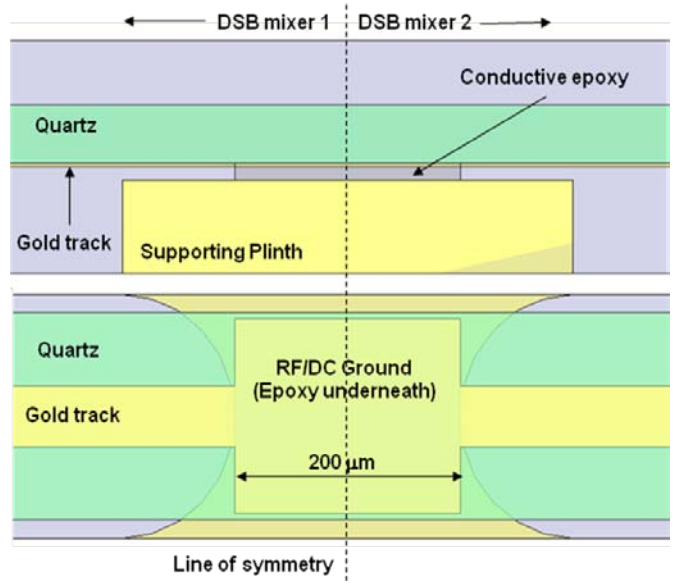

Fig. 6: Geometry of RF/DC Ground Point: side view (upper), plan view (lower).

Waveguide Load Return Loss Tests

Return loss measurements were performed on an ABmm VNA. Waveguide calibration kits from Radiometer Physics GmbH were employed in each frequency band to ensure an accurate reference. Measurements were performed from 150-190 GHz and 310-360 GHz covering the LO and RF bandwidths of the SHIRM devices. Fig. 7 presents the return loss results for each of the three waveguide load designs manufactured from MF-116 across the band 150-190 GHz. The MF-116 material was found to be superior for all geometries hence the MF-112 results have been omitted. Furthermore, each load was found to have similar return loss performance across the 310-360 GHz band. For brevity, these results are not shown.

Fig. 7 shows that the performance of the initial incorrectly shaped load design is poor, with a typical return loss of -10 dB. The other two designs show a marked improvement with a return loss better than -20 dB across the band. The poor performance of the initial design is attributed to the geometry of the taper in relation to the incident electric field.

SHIRM Test Results with Improved Waveguide Loads

Load 2 designs were retro-fitted into each of the SHIRM units and identical tests were undertaken to determine the improvement in performance. Fig. 8 presents the results of the sideband rejection tests of SHIRM A for the same LO frequencies and IF bandwidths as presented in Fig. 4. Comparing the figures it can be seen that the sideband rejection has improved, whilst the relative levels of sideband rejection for the three LO frequencies remains the same. Best performance is still achieved at LO=174 GHz were the average level of sideband rejection is 25.2 dB (R_{LSB}) and 26.2 dB (R_{USB}), a mean improvement of 6.4 dB. Poorest performance is again at LO=170 GHz were the average level of sideband rejection is 14.8 dB (R_{LSB}) and 14.6 dB (R_{USB}), a mean improvement of 3.4 dB.

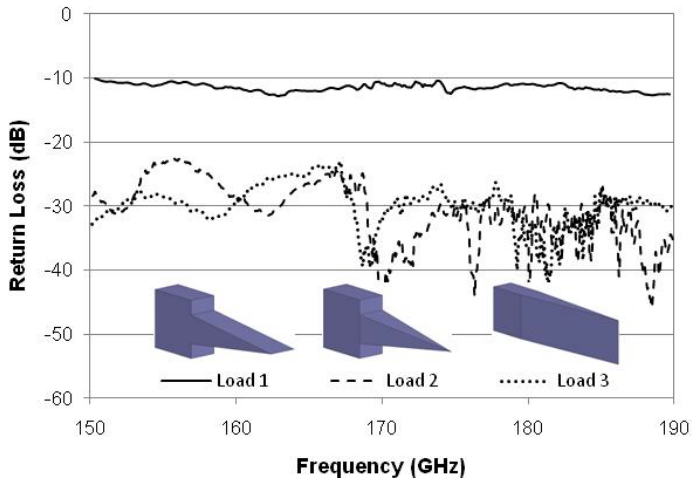

Fig. 7: Measured Return Loss of Waveguide Load Geometries from 150-190 GHz: Load 1, H-plane taper (initial design); Load 2, double taper; Load 3, E-plane taper.

A SSB receiver noise temperature between 3150-3600 K and 3800-5050 K was achieved for IF bandwidths of 2-8 GHz and 6-14 GHz respectively. SHIRM A provides >20 dB of sideband rejection over the majority of both sidebands at LO=174 GHz. Although the new load has improved performance, the relative variation in performance between LO frequencies remains. This effect is dominated by the amplitude and phase imbalance of the LO splitting/phase shifting network over the broad bandwidth of operation.

Fig. 9 presents the results of the sideband rejection tests of SHIRM B for the same LO frequencies and IF bandwidths as presented in Fig. 5. Comparing the figures it can be seen that the sharp degradation is sideband rejection with LO frequency has been eliminated and significantly improved performance has been achieved at LO=167 GHz and LO=168 GHz. Best performance is achieved at LO=168 GHz were the average level of sideband rejection is 26.1 dB (R_{LSB}) and 19.1 dB (R_{USB}). A SSB receiver noise temperature between 3000-3350 K and 4100-5000 K was achieved for IF bandwidths of 2-8 GHz and 6-14 GHz respectively.

The best performance achieved to date for each SHIRM topology is summarized in Table I.

TABLE I
Summary of Best SHIRM Performance (IF Bandwidth = 2-14 GHz)

LO (GHz)	R_{LSB} (dB)			R_{USB} (dB)			T_{SSB} (K)	
	Min	Max	Ave	Min	Max	Ave	Min[1]	Max[2]
SHIRM A								
174	18.7	34.9	25.2	19.7	30.4	26.2	3500	4800
SHIRM B								
168	17.5	35.3	26.1	16.1	25.9	19.1	3000	5000

[1]Minimum T_{SSB} achieved at 2-8 GHz IF bandwidth, T_{IF}=70 K.

[2]Maximum T_{SSB} achieved at 6-14 GHz IF bandwidth, T_{IF}=133 K.

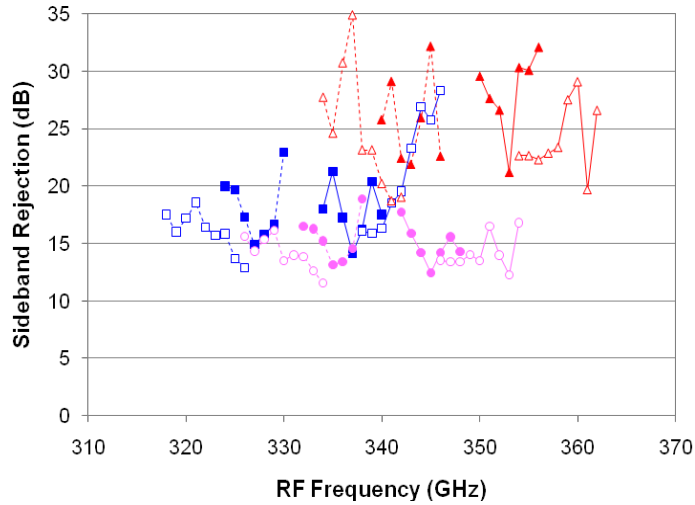

Fig. 8: Measured Sideband Rejection Performance of SHIRM A with Waveguide Load 2 as a Function of RF Freqeuncy. Filled markers IF=2-8 GHz, empty markers IF=6-14 GHz. Dotted lines show R_{LSB} and continuous lines show R_{USB}. Blue square markers for LO=166 GHz, pink round markers for LO=170 GHz, red triagular markers for LO=174 GHz.

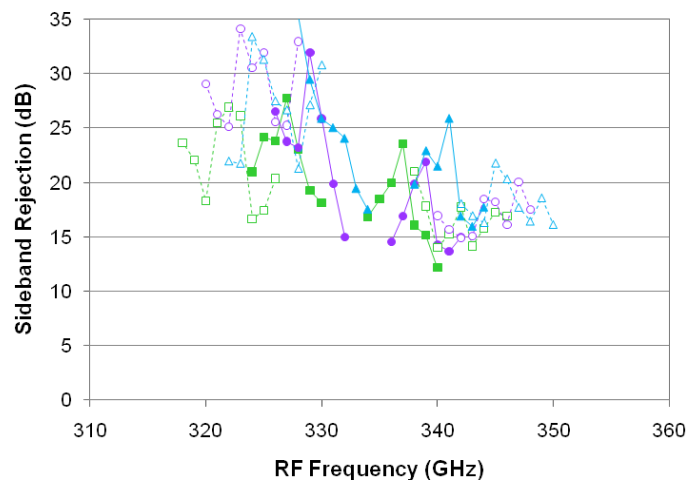

Fig. 9: Measured Sideband Rejection Performance of SHIRM B with Waveguide Load 2 as a Function of RF Freqeuncy. Filled markers IF=2-8 GHz, empty markers IF=6-14 GHz. Dotted lines show R_{LSB} and continuous lines show R_{USB}. Green square markers for LO=166 GHz, purple round markers for LO=167 GHz, indigo triagular markers for LO=168 GHz.

VI. Effect of Asymmetrical RF/DC Ground

The geometry of the RF/DC ground point in the middle of the centre quartz line was presented in Fig. 6 and discussed in Section IV. The electrical connection between the gold track of the microstrip transmission line and the supporting plinth is made by applying conductive epoxy to the plinth before positioning the quartz centre line and curing the epoxy at the lowest possible temperature to minimize thermal expansion. The phase imbalance created by an asymmetry in the epoxy join has been simulated over the LO and RF bandwidths. The asymmetry has been created by modeling different lengths of epoxy extending from each side of the line of symmetry. The phase imbalance is then calculated as the difference in reflection phase from each side of the short. Fig. 10 shows the

phase imbalance introduced for length differences of 0, 20, 40, 60 and 80 μm. As expected the phase imbalance increases with frequency (decreasing wavelength) and is therefore more significant over the RF bandwidth. Comparing the phase imbalance introduced by an asymmetrical join and the maximum phase imbalance of the SHIRM A IQ mixer block measured using the digital correlator backend, it is evident that an asymmetrical join has the potential to be a major source of imbalance.

In an effort to try and eliminate any asymmetry at the RF/DC ground point, a new method for creating the ground using beam-leads is being implemented. The geometry of this method is presented in Fig. 11. Here, beam-leads extend from the side of the quartz beyond the edge of the waveguide channel making an electrical connection with the block. Non-conductive glue is used to fix the centre quartz line to the supporting plinth. The supporting plinth has been raised slightly to account for the expected thinner layer of glue as opposed to the thicker layer of conductive epoxy. Development of the SHIRM employing this grounding method is on-going.

VII. Conclusions

An improvement in the level of sideband rejection of two SHIRM topologies has been achieved by incorporating improved waveguide loads in the isolated ports of the integrated quadrature hybrids of the IQ mixer blocks. The improved loads have also eliminated the problem of a sharp degradation in sideband rejection performance with small changes in LO frequency. This was especially prevalent in SHIRM B. SHIRM A has achieved a sideband rejection >18.7 dB at LO=174 GHz and SHIRM B has achieved a sideband rejection >16.1 dB at 168 GHz, both over a broad IF bandwidth of 2-14 GHz.

Ongoing efforts to further improve performance are focused on implementing a new RF/DC ground point to minimize any asymmetry that may be introduced by the current grounding method employing conductive epoxy.

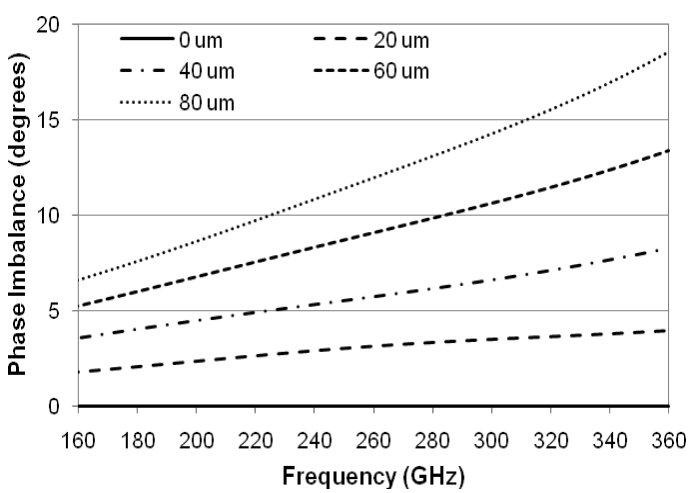

Fig. 10: Phase imbalance introduced due to asymmetrical conductive epoxy joint.

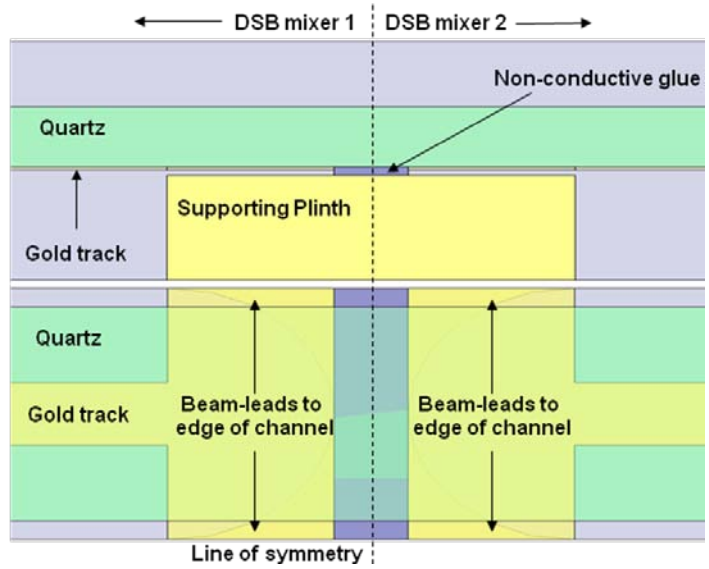

Fig. 11: Geometry of new RF/DC Ground Point using Beam-leads: side view (upper), plan view (lower).

References

[1] B. Thomas, S. P. Rea, B. Moyna, D. N. Matheson, "Development of a 340-GHz Sub-Harmonic Image Rejection Mixer Using Planar Schottky Diodes," *ISSTT*, Groningen, Holland, 2008.

[2] S. P. Rea, B. Thomas, D. N. Matheson, "A 320-360 GHz Sub-Harmonically Pumped Image-Rejection Mixer for Earth Observation Applications," *33rd International Conference on Infrared, Millimetre and Terahertz Waves*, California, USA, 2008.

[3] B. Thomas, S. P. Rea, B. Moyna, B. Alderman, D. Matheson, "A 320–360 GHz Sub-harmonically Pumped Image Rejection Mixer Using Planar Schottky Diodes" *IEEE Microwave and Wireless Components Letters*, Vol. 19, No. 2, Feb. 2009, pp. 101–103.

[4] P. Sobis, J. Stake, A. Emrich, "Towards a THz Sideband Separating Subharmonic Schottky Mixer," *ISSTT*, Groningen, Holland, 2008.

[5] P. Sobis, T. Bryllert, A. Ø. Olsen, J. Vukusic, V. Drakinskiy, S. Cherednichenko, J. Stake, A. Emrich, "Development of a Compact 340 GHz Receiver Front-End," *5th ESA Workshop on Millimetre Wave Technology and Applications & 31st ESA Antenna Workshop*, Noordwijk, Holland, 2009.

[6] F. V. Scheele, *et al.*, "The STEAM Project," *Proceedings of the Committee On Space Research, COSPAR*, Paris, France, pp. 2208, July 2004.

[7] J. Langen, P. Bensi, D. Lamarre, U. Frisk, "PREMIER – PRocess Exploration through Measurements of Infrared and millimetre-wave Emitted Radiation," *ESA SP-1313/5 Candidate Earth Explorer Core Missions Reports for Assessment*, ISBN 978-92-9221-406-7, European Space Agency, 2008.

[8] B. Alderman, H. Sanghera, C. Price, B. Thomas, D. N. Matheson, "Fabrication of Reproducible Air-bridged Schottky Diodes for use at Frequencies near 200 GHz," *Proceedings of the joint 32nd IR and MM-wave conference and 15th THz Electronics 2007*, Cardiff, September 2007, pp. 848-849.

[9] A. R. Kerr, S-K. Pan, J. E. Effland, "Sideband Calibration of Millimeter-Wave Receivers," *ALMA Memo 357*, Mar. 2001.

[10] P. G. Huggard, B. N. Ellison, P. Shen, N. J. Gomes, P. A. Davies, W. Shillue, A. Vaccari, J. M. Payne, "Generation of millimetre and sub-millimetre waves by photomixing in 1.55 μm wavelength photodiode", *Electronics Letters*, 38, 2002, pp. 327-328.

[11] A. Murk, J. Treuttel, S. P. Rea, D. N. Matheson, "Characterization of a 340 GHz Sub-Harmonic IQ Mixer with Digital Sideband Separating Backend," *5th ESA Workshop on Millimetre Wave Technology and Applications & 31st ESA Antenna Workshop*, Noordwijk, Holland, 2009.

[12] A. R. Kerr, H. Moseley, E. Wollack, W. Grammer, G. Reiland, R. Henry, K. P. Stewart, "MF-112 and MF-116: Compact Waveguide Loads and FTS Measurements at Room Temperature and 5K," *ALMA Memo 494*, May, 2004.